



**ADVANCES IN
FOREST FIRE
RESEARCH**

DOMINGOS XAVIER VIEGAS

EDITOR

2014

Time series of land surface temperature from daily MODIS measurements for the prediction of fire hazard

Carmine Maffei, Silvia Alfieri, Massimo Menenti

^aDelft University of Technology, Stevinweg 1, 2628 CN, Delft, Netherlands, c.maffei@tudelft.nl, s.m.alfieri-1@tudelft.nl, m.menenti@tudelft.nl

Abstract

Prolonged heat and absence of rainfall drive vegetation into water stress conditions that lead to an increase of its temperature. Since stressed vegetation is more prone to fire, it is expected that remote sensing mapping of temperature anomalies might be a viable tool to predict fire hazard. The identification of these anomalies requires the prior definition of a reference temperature against which compare actual recorded temperatures. This can be achieved by using long time series of satellite data and the HANTS (Harmonic ANalysis of Time Series) algorithm. The objective of this research was the characterisation of fire hazard using temporal series of land surface temperature (LST) derived from Terra-MODIS measurements. The investigation was based on a sequence of MODIS LST data from 2000 to 2008 in Campania (13595 km²), Italy, and on a data set of 7700 fires recorded in the area in the same period. Missing and/or cloudy LST data were reconstructed by means of the HANTS algorithm applied to annual sequences of daily observations. The coefficients of the Fourier analysis were assessed against spatial patterns of fire occurrence. HANTS algorithm was also used to construct daily reference temperature maps against which to evaluate temperature anomalies and cumulated temperature anomalies. Results show that fires tend to occur in areas characterised by specific values of several Fourier coefficients with high significance, and to avoid the other areas. The amplitude of the second harmonic is the only Fourier coefficient dictating mean fire size. The mean fire size and the proportion of large fires correlate with both daily and cumulated thermal anomalies.

Keywords: *Land surface temperature; MODIS; Time series; HANTS; Fire hazard.*

1. Introduction

Prolonged heat and absence of rainfall drive vegetation into water stress conditions that lead to an increase of its temperature. Since stressed vegetation is more prone to fire, there might be a potential role for Earth observation technologies in mapping fire hazard (Leblon 2005), whereas it is proved that current orbiting instruments are able to detect anomalies in vegetation temperature.

The identification of temperature anomalies requires the prior definition of a reference temperature against which compare actual recorded temperature. By using long time series of satellite data it is possible to identify expected temporal patterns on a pixel-by-pixel basis. The HANTS (Harmonic ANalysis of Time Series) algorithm accomplishes this task by means of a Fourier series (Verhoef *et al.* 1996). HANTS has been reported to successfully provide reference data for both vegetation spectral indexes and land surface temperature (Julien *et al.* 2006).

The objective of this research was to develop and test a methodology for the characterisation of fire hazard from anomalies of daily land surface temperature (LST), as derived from thermal infrared measurements of the Moderate Resolution Imaging Spectrometer (MODIS) on board Terra satellite, evaluated against a reference temperature calculated with HANTS algorithm. Since maps of HANTS coefficients provide a detailed characterisation of the spatial and temporal pattern of surface temperatures, their potential to explain spatial patterns of fire occurrence was also investigated.

2. Materials and methods

2.1. Study area

The research focussed on Campania (13595 km²), Italy. The Italian Forest Corps (*Corpo Forestale dello Stato*) provided a dataset of more than 7700 fire records covering years between 2000 and 2008. Data included date and time, coordinates, duration and extent of each event.

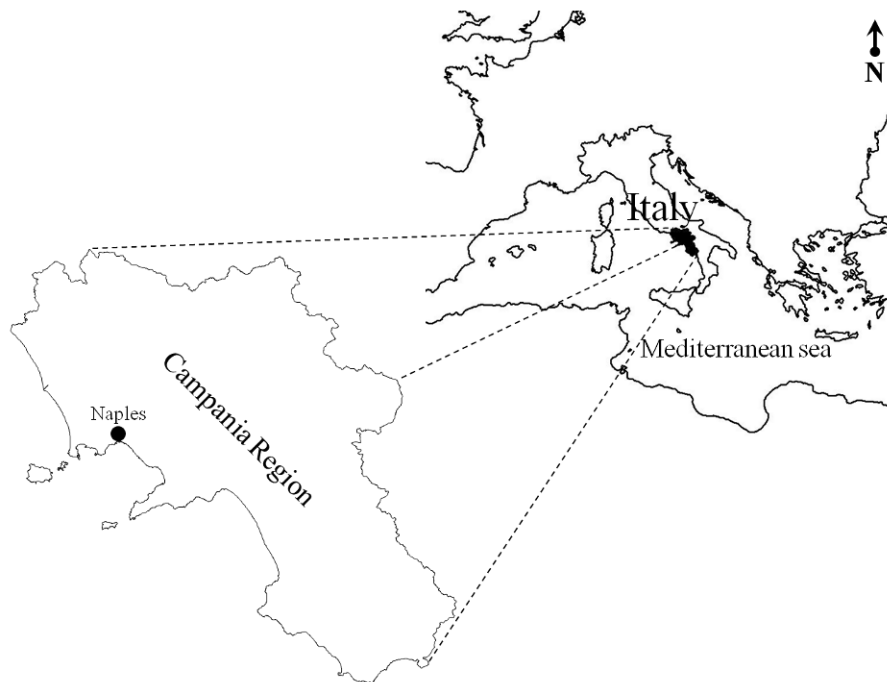


Figure 1. Study area.

2.2. MODIS land surface temperature data

A collection of daily diurnal (approximately 10.30 am local time) Terra-MODIS LST data from 2000 to 2008 was used for this research. These data are publicly available at the Land Processes Distributed Active Archive Center (“LP DAAC”) hosted by the United States Geological Survey (USGS).

2.3. Fourier analysis of LST data

Series comprising three harmonics (365, 180 and 120 days) were fit to the data with two different methods, to achieve the diverse purposes of this research:

- HANTS was executed on each yearly sequence of daily LST data separately, to reconstruct missing or cloudy data (Roerink *et al.* 2000). The retrieved yearly images of Fourier coefficients (mean LST, amplitude and phase of the three harmonics) were then compared against spatial patterns of fire occurrence.
- The algorithm was executed on the whole 2000-2008 dataset to construct daily maps of reference temperature (Azzali and Menenti 1999). These served as a basis for the calculation of thermal anomalies.

2.4. Spatial patterns of fire occurrence

Yearly maps of Fourier coefficients were masked on forest and natural areas (as from the CORINE Land Cover 2000 map) and segmented into labelled classes. Masking was performed to ensure

consistency between the characteristics of the database, which includes only fires occurred in forests and other natural areas, and further analyses based on the spatial distribution of fires.

Spatial patterns of fire occurrence were assessed with respect to fire number and mean burnt area in terms of selectivity, i.e. by understanding whether in each class fire incidence is higher (preferred) or lower (avoided) than expected from a random null model (Bajocco and Ricotta 2007).

2.5. Analysis of LST anomalies

Daily maps of thermal anomalies (TA) were computed by subtracting the daily reference temperature from MODIS LST. Forest fires are expected to occur in areas where there has been a prolonged exposure to lack of rainfall and high air temperature. In these circumstances a temperature anomaly is observed over a number of consecutive days. For this reason cumulated anomalies (CTA) were calculated as the sum of all the observed thermal anomalies from the day when the thermal anomaly was first recorded in the pixel up to the current day. Each fire in the database was then associated to the values of TA and CTA observed at fire's location in the day previous to the event.

3. Results

The mean annual temperature and the amplitudes of the three harmonics used in the analysis have an evident role in determining spatial patterns of fire occurrence (Tables 1 to 4). Among the phase components, fire occurrence shows clear spatial selectivity only against the first (Table 5, other tables not shown). Mean fire size shows unambiguous spatial selectivity solely in the amplitude of the second harmonic (Table 3).

Temperature anomalies and cumulated temperature anomalies were evaluated against fire size by first calculating the conditional mean fire size observed when the TA (CTA) was larger of the considered value, and then plotting the calculated means against the values of anomaly (cumulated anomaly) used in the calculation. In a similar manner, the conditional proportion of large fires (larger than 16 ha, which is the 90th percentile in the study area) was evaluated against anomaly and cumulated anomaly.

Table 1. Selectivity of fires' number and mean size for mean temperature classes. Symbol "+" means class preference, "-" class avoidance. One symbol: selectivity non significant. Two symbols: significant $P < 0.05$. Three symbols: significant $P < 0.01$.

| Constant component of Fourier analysis (K) | | | | |
|--|-----------------|-----|----------------|-----|
| Class | Number of fires | | Mean fire size | |
| <288 | 34 | --- | 15,74 | +++ |
| 288-289 | 47 | --- | 7,09 | +++ |
| 289-290 | 121 | -- | 5,39 | + |
| 290-291 | 264 | +++ | 7,34 | + |
| 291-292 | 494 | +++ | 4,4 | - |
| 292-293 | 782 | +++ | 4,23 | - |
| 293-294 | 904 | +++ | 4,85 | - |
| 294-295 | 751 | +++ | 3,99 | -- |
| 295-296 | 560 | - | 5,52 | + |
| 296-297 | 279 | --- | 4,81 | + |
| 297-298 | 127 | --- | 9,67 | +++ |
| >298 | 41 | --- | 4,79 | + |

Table 2. Selectivity of fires' number and mean size for classes of amplitude of the first harmonic. Symbol "+" means class preference, "-" class avoidance. One symbol: selectivity non significant. Two symbols: significant $P < 0.05$. Three symbols: significant $P < 0.01$.

| Amplitude of the first harmonic (K) | | | | |
|-------------------------------------|-----------------|-----|----------------|-----|
| Class | Number of fires | | Mean fire size | |
| <8 | 59 | - | 7,79 | + |
| 8-9 | 203 | + | 4,97 | + |
| 9-10 | 453 | +++ | 5,8 | + |
| 10-11 | 984 | +++ | 4,55 | - |
| 11-12 | 1242 | +++ | 4,94 | + |
| 12-13 | 872 | --- | 4,71 | - |
| 13-14 | 411 | --- | 4,39 | - |
| 14-15 | 158 | --- | 6,02 | + |
| >15 | 22 | --- | 27,05 | +++ |

Table 3. Selectivity of fires' number and mean size for classes of amplitude of the second harmonic. Symbol "+" means class preference, "-" class avoidance. One symbol: selectivity non significant. Two symbols: significant $P < 0.05$. Three symbols: significant $P < 0.01$.

| Amplitude of the second harmonic (K) | | | | |
|--------------------------------------|-----------------|-----|----------------|-----|
| Class | Number of fires | | Mean fire size | |
| 0-1 | 2083 | +++ | 3,52 | --- |
| 1-2 | 1723 | + | 6,01 | +++ |
| 2-3 | 570 | --- | 7,24 | +++ |
| >3 | 28 | --- | 12,85 | +++ |

Table 4. Selectivity of fires' number and mean size for classes of amplitude of the third harmonic. Symbol "+" means class preference, "-" class avoidance. One symbol: selectivity non significant. Two symbols: significant $P < 0.05$. Three symbols: significant $P < 0.01$.

| Amplitude of the third harmonic (K) | | | | |
|-------------------------------------|-----------------|-----|----------------|---|
| Class | Number of fires | | Mean fire size | |
| 0-1 | 1486 | +++ | 5,06 | + |
| 1-2 | 2450 | +++ | 4,99 | - |
| 2-3 | 447 | --- | 5,2 | + |
| >3 | 21 | --- | 4,88 | + |

Table 5. Selectivity of fires' number and mean size for classes of phase of the first harmonic. Symbol "+" means class preference, "-" class avoidance. One symbol: selectivity non significant. Two symbols: significant $P < 0.05$. Three symbols: significant $P < 0.01$.

| Phase of the first harmonic (°) | | | | |
|---------------------------------|-----------------|-----|----------------|-----|
| Class | Number of fires | | Mean fire size | |
| <180 | 21 | --- | 10,15 | ++ |
| 180-185 | 126 | --- | 3,12 | --- |
| 185-190 | 645 | --- | 3,21 | --- |
| 190-195 | 1438 | +++ | 4,29 | -- |
| 195-200 | 1329 | +++ | 6,63 | +++ |
| 200-205 | 623 | ++ | 5,28 | + |
| 205-210 | 193 | +++ | 5,27 | + |
| >210 | 29 | + | 6,9 | + |

Daily thermal anomalies appear to be related to fire size: with increasing values of the thermal anomaly, the expected mean fire size in all areas with thermal anomaly larger of that value increases (Figure 2, left). A similar pattern is observed with the conditional fraction of large fires (Figure 2, right). A wider dynamic range in fire size and fraction of large fires is observed when the same analysis is performed against CTA (Figure 3).

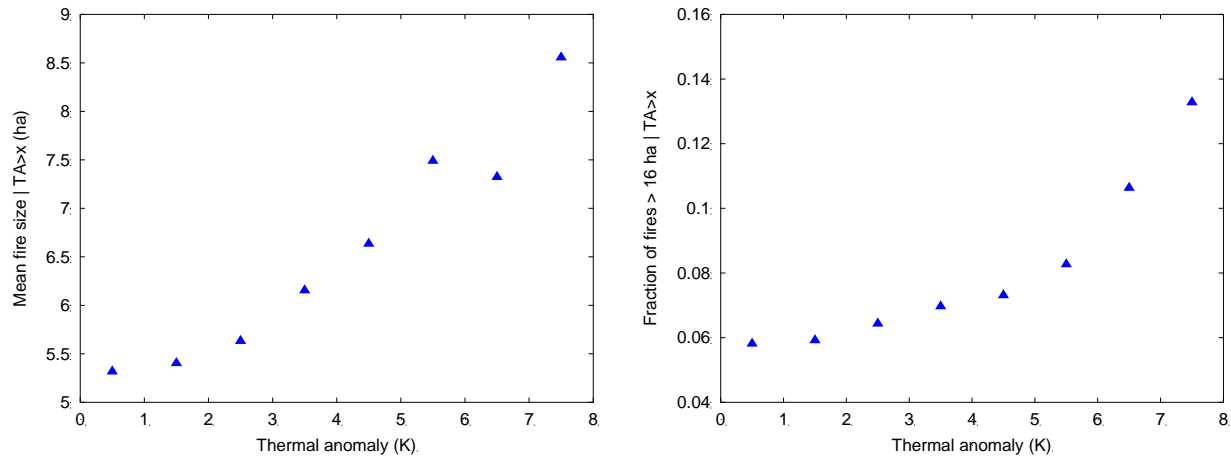


Figure 2. Relationship between conditional mean fire size (left) and conditional fraction of large fires (right) against values of thermal anomaly (TA) observed in the day previous to the event at fires' locations.

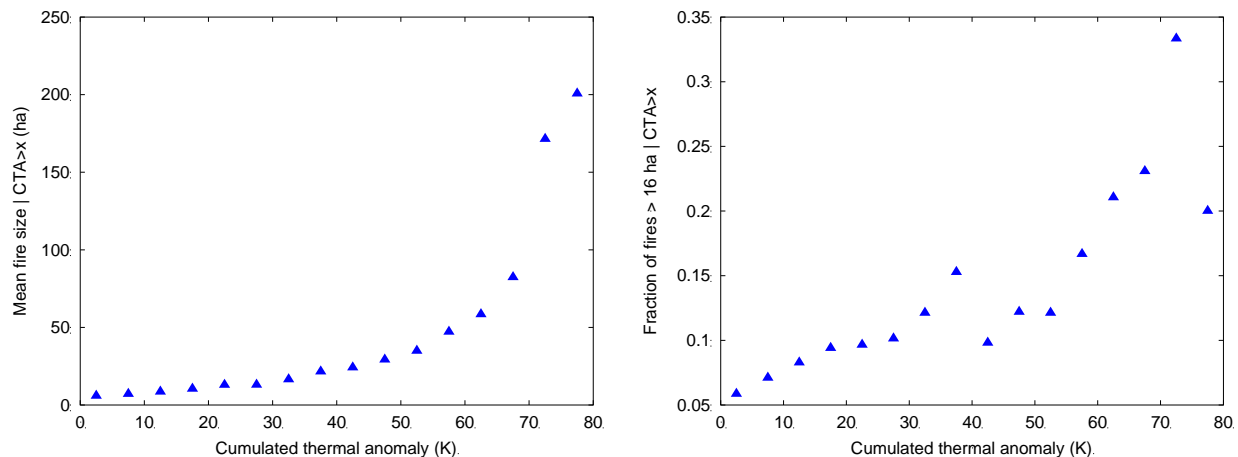


Figure 3. Relationship between conditional mean fire size (left) and conditional fraction of large fires (right) against values of cumulated thermal anomaly (CTA) observed in the day previous to the event at fires' locations.

4. Discussion

Results show that the HANTS algorithm plays an important role in both characterising spatial patterns of fire occurrence and in predicting mean fire size. Indeed, fires occurrence shows clear selectivity against mean value, amplitude of the three harmonics and phase of the first harmonic of LST computed on a yearly basis. Mean fire size shows selectivity only against the amplitude of the second harmonic. Here, a clear inverse relationship between number of fires and mean fire size is observed, with larger fires significantly preferring areas where the amplitude is larger (Table 3).

The only phase component of the Fourier analysis related to fires incidence is that of the first harmonic; fires significantly prefer areas where this phase is higher. The phase carries information on the timing

of fire events, and indeed a larger number of fires is observed where the phase is higher, i.e. when a prolonged warm season occurs.

A relationship was found between conditional mean fire size and thermal anomalies (Figure 2). With increasing values of the thermal anomaly, the conditional mean fire size increases. A similar trend is observed with the conditional fraction of fires larger than 16 ha. From the point of view of fire size, cumulated thermal anomaly maps carry a stronger informative content. CTA is a measure of heat “accumulated” in a certain area, providing more direct information on the prolonged exposure of vegetation to stress conditions. This is reflected in the prediction of expected mean fire size over two orders of magnitude (Figure 3). Moreover, when the cumulated anomaly is larger than about 60 K, a steep increase in mean fire size is observed, potentially allowing the production of more meaningful fire hazard maps as compared to TA.

5. Acknowledgements

We are grateful to the Forest Fires office of the Italian Forest Corps (CFS) and the Italian Civil Protection for providing fire data in the study area.

6. References

- Azzali S, Menenti M (1999) Mapping isogrowth zones on continental scale using temporal Fourier analysis of AVHRR-NDVI data. *Int J Appl Earth Obs Geoinf* 1(1), 9–20. doi:10.1016/S0303-2434(99)85023-5.
- Bajocco S, Ricotta C (2007) Evidence of selective burning in Sardinia (Italy): which land-cover classes do wildfires prefer? *Landsc Ecol* 23(2), 241–248. doi:10.1007/s10980-007-9176-5.
- Julien Y, Sobrino JA, Verhoef W (2006) Changes in land surface temperatures and NDVI values over Europe between 1982 and 1999. *Remote Sens Environ* 103, 43–55. doi:10.1016/j.rse.2006.03.011.
- Leblon B (2005) Monitoring Forest Fire Danger with Remote Sensing. *Nat Hazards* 35(3), 343–359. doi:10.1007/s11069-004-1796-3.
- LP DAAC <https://lpdaac.usgs.gov/>. Accessed 26 June 2014.
- Roerink GJ, Menenti M, Verhoef W (2000) Reconstructing cloudfree NDVI composites using Fourier analysis of time series. *Int J Remote Sens* 21(9), 1911–1917. doi:10.1080/014311600209814.
- Verhoef W, Menenti M, Azzali S (1996) A colour composite of NOAA-AVHRR-NDVI based on time series analysis (1981-1992). *Int J Remote Sens* 17, 231–235. doi:10.1080/01431169608949001.